Nanoscale

PAPER

View Article Online
View Journal | View Issue

Cite this: *Nanoscale*, 2016, **8**, 15281

One-step microwave synthesis of N-doped hydroxyl-functionalized carbon dots with ultra-high fluorescence quantum yields†

Yongqiang Zhang,[a,b] Xingyuan Liu,*[a] Yi Fan,[a] Xiaoyang Guo,[a] Lei Zhou,*[c] Ying Lv[a] and Jie Lin*[a]

Received 16th April 2016,
Accepted 26th July 2016

DOI: 10.1039/c6nr03125k

www.rsc.org/nanoscale

A one-step microwave synthesis of N-doped hydroxyl-functionalized carbon dots (CDs) with ultra-high fluorescence quantum yields (QYs) of 99% is reported. These ultra-high QY CDs were synthesized using citric acid and amino compound-containing hydroxyls like ethanolamine and tris(hydroxylmethyl)aminomethane. Amino and carboxyl moieties can form amides through dehydration condensation reactions, and these amides act as bridges between carboxyl and hydroxyl groups, and modify hydroxyl groups on the surface of the CDs. The entire reaction can be carried out within 5 min. When the molar ratio of reactants is 1 : 1, the hydroxyl and graphitic nitrogen content is the highest, and the synergy leads to a high ratio between the radiative transition rate and nonradiative transition rate as well as a high QY. The developed pathway to N-doped hydroxyl-functionalized CDs can provide unambiguous and remarkable insights into the design of highly luminescent functionalized carbon dots, and expedite the applications of CDs.

Introduction

As a fluorescent material, carbon nanodots (CDs) have important applications in photocatalysis,[1] sensors,[2] lasers,[3] LEDs,[4] photovoltaic devices,[5] bio-imaging,[6] and photodetectors.[7] Fluorescence quantum yield (QY) is an important attribute to judge whether a material is a good luminous material, and it serves as an important basis for the practical applications of the material. To enhance their performance and exploit other potential applications, facile and efficient strategies towards the synthesis of CDs with high QYs are desired.[8] A host of methods to improve the fluorescence QY of CDs have been reported, such as chemical reduction,[8c,9] photochemical reduction,[8b] surface passivation,[10] and modification.[9b] However, these methods often require long reaction times as well as the use of toxic reagents, such as $NaBH_4$, $N_2H_4{\cdot}H_2O$, and alkylamines among others. It is well known that hydroxyl groups are strong electron-donating substituents, and can greatly enhance the QYs of luminescent centers.[8b,11] Reduction reactions are needed to acquire hydroxyl-functionalized CDs. Zheng, Zhu, and Yang *et al.* illustrated that hydroxyl-functionalized CDs obtained by chemical reduction exhibited decent QYs;[8c,9] however, the QY of hydroxyl-functionalized CDs has not exceeded 50% to date. Recently, Yang and Sun *et al.* demonstrated that N-doping with amino compounds can greatly improve the QY of select compounds; specifically, high QYs of 80% and 94% were obtained from hydrothermally synthesized N-doped CDs.[2a,12] However, the raw materials were confined to citric acid (CA) and toxic ethylenediamine (ED). Furthermore, hydrothermal synthesis requires several hours and dangerous conditions including high temperatures and pressures. To date, there are few reports on highly luminescent CDs. Therefore, universal, facile strategies for the synthesis of luminescent CDs with high QYs are greatly needed.

Herein, we report the synthesis of a series of CDs with ultra-high QYs (denoted as Tris-CDs and EA-CDs) using a one-step microwave process through the dehydration condensation of the carboxyl group in CA and amino compounds containing hydroxyl groups like tris(hydroxylmethyl)aminomethane (abbreviated as Tris) and ethanolamine (EA); the hydroxyl group was subsequently modified on the surface of the CDs. The entire reaction can be carried out within 5 min. Tris-CDs were synthesized from CA and Tris, while EA-CDs were synthesized from CA and ethanolamine (EA). The QY of Tris-CD (1 : 1) (where the molar ratio of CA : Tris was 1 : 1) was 99.3%, as determined by a slope method (Fig. S1 and Table S1†), and the QY of EA-CD (1 : 1) was 96.3% (Fig. S2 and Table S2†).

[a]*State Key Laboratory of Luminescence and Applications, Changchun Institute of Optics, Fine Mechanics and Physics, Chinese Academy of Sciences, Changchun 130033, China. E-mail: liuxy@ciomp.ac.cn, linj@ciomp.ac.cn*
[b]*University of Chinese Academy of Sciences, Beijing, 100049, China*
[c]*State Key Laboratory of Pathogen and Biosecurity, Beijing Institute of Microbiology and Epidemiology, Beijing 100071, China. E-mail: ammszhoulei@aliyun.com*

†Electronic supplementary information (ESI) available. See DOI: 10.1039/c6nr03125k

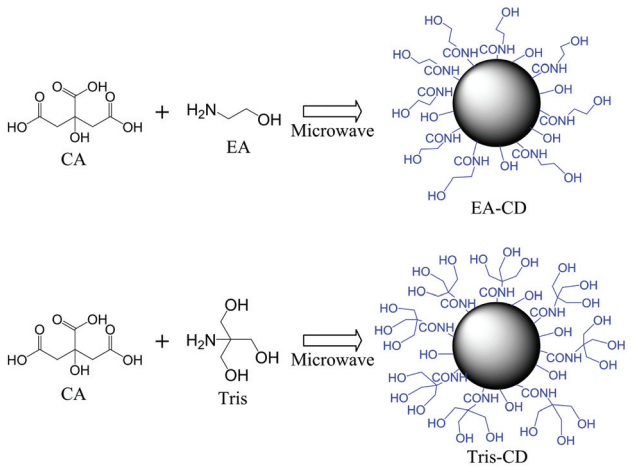

Scheme 1 Synthesis of EA-CDs and Tris-CDs.

We also demonstrate that surface hydroxyl groups and graphite-N can largely improve the QY. Our work provides a simple and green pathway to synthesize highly luminescent CDs.

Our strategy is based on the dehydration condensation reaction between carboxyl and amino groups; the approach is depicted in Scheme 1. Typically, a graphite framework can be formed through the intermolecular dehydration condensation of CA, and compounds containing amino groups, such as ED or urea could be fixed on the graphite framework structure through dehydration condensation to fabricate N-doped CDs.[13] In microwave synthesis, CA and alcohols, such as ethanol, ethylene glycol, and 1,1,1-tris(hydroxylmethyl)ethane cannot form CDs, as carbonization did not occur and fluorescence was not detected in an aqueous solution of the products. On the other hand, CA and amines can react to fabricate N-doped CDs, so when amino compounds are replaced with amino-hydroxyls in the reaction, the hydroxyls can be modified on the surface of the CDs. Carboxyl groups react faster with amino groups than hydroxyl groups due to the facile protonation of amino groups. The resulting CDs combine the advantages of both N-doped CDs and hydroxyl-functionalized CDs, and exhibit ultra-high QYs.

Experimental section

Experimental materials

Citric acid monohydrate, ethanol, ethylenediamine (ED), ethylene glycol, ethanolamine (EA), and tris(hydroxylmethyl)aminomethane (Tris) were purchased from Sinopharm Chemical Reagent Co., Ltd. 1,1,1-Tris(hydroxylmethyl)ethane was purchased from Aladdin Industrial Corporation. All chemicals were of analytical grade and were used as received without further purification. Ultrapure water was obtained by purification using a Millipore system and was used in all experiments.

Synthesis of ED-CD

Various molar ratios of CA and ED were added to 20 mL of distilled water, and sonicated until transparent solutions were formed. The solutions were transferred into a domestic 700 W microwave oven and heated under 350 W (medium heat) for 5 min (the heating curve is shown in Fig. S3†). The first three heating periods were carried out to remove water quickly, and regular intervals are needed to avoid bumping. The following short heating period was carried out to prevent uneven carbonization caused by rapid heating, and the other heating periods were required for further carbonization of the unreacted polymeric structures. Stirring and shaking were necessary during these intervals to ensure a homogeneous reaction. The final products were collected by adding ultrapure water to the aqueous solutions and centrifuging at 5000 rpm (1660*g*) for 5 min to precipitate aggregates. Then, the supernatant was further purified using a 0.02 μm filter (GE Whatman, Anotop). Then it was freeze-dried to powder and collected. The obtained CDs were denoted as ED-CD (1 : *x*), where *x* stands for the molar ratio of ED to CA (the molar ratio of ED per mole of CA); for example, CDs prepared with 3.5 g (1/60 mol) CA and 0.33 mL (0.3/60 mol) were denoted as ED-CD (1 : 0.3).

Synthesis of EA-CD

Various molar ratios of CA and EA were added to 20 mL of distilled water, and followed the procedure for the synthesis of ED-CD. The resulting CDs were weighed and divided by the weight of the precursors, then the yields were calculated and are shown in Table S3 and Fig. S4.†

Synthesis of Tris-CD

A series of various molar ratios of CA and Tris were added to 20 mL distilled water, and followed the procedure for the synthesis of ED-CD. The resulting CDs were weighed and divided by the weight of the precursors, then the yields were calculated and are shown in Table S3 and Fig. S4.†

Characterization

High-resolution TEM (HR-TEM) images and fast Fourier transform (FFT) spot diagrams were recorded using a FEI-TECNAI G2 transmission electron microscope (TEM) operated at 200 kV. The powder X-ray diffraction (XRD) pattern was collected on a Bruker D8 Focus diffractometer, in the 2θ range from 10° to 60° with Cu Kα radiation (λ = 1.54056 Å) operated at 40 kV and 30 mA, and the increment was 0.02° and the scan-speed was 0.5 s (scanning time on each increment). X-Ray photoelectron spectra (XPS) were obtained using a Thermo Scientific ESCALAB 250 with Multitechnique Surface Analysis. Fourier Transform Infrared (FT-IR) spectra of Tris-CD (1 : 1) were recorded using KBr tablets with a Bio-Rad Excalibur FTS3000 spectrometer (4000–1000 cm^{-1}). UV-Vis absorption spectra were obtained using a Shimadzu UV-3101 PC scanning spectrometer. Fluorescence emission spectra were recorded on a Hitachi fluorescence spectrophotometer F-7000. Fluorescence lifetimes were measured using a FLS920 time-

corrected single photon counting system. Centrifugation was done using a TGL-16G centrifuge. Zeta potentials were measured on a Malvern Zetasizer Nano ZS. Confocal fluorescence microscopy images were obtained using an Olympus FV1000 confocal laser scanning microscope.

Results and discussion

Morphology and chemical structure investigations

Transmission electron microscopy (TEM) (Fig. 1a) revealed that Tris-CDs (1 : 1) were torispherical and uniformly distributed without aggregation. HR-TEM (upper inset picture of Fig. 1a) revealed a lattice spacing distance of 2.1 Å, which corresponds to the in-plane lattice spacing of graphite (100 facet).[8a] The lower inset of Fig. 1a shows the size distribution histogram of Tris-CD (1 : 1), which varied from 0.8 to 2.1 nm with a mean value of around 1.34 nm, which is smaller than that of other reports. The size distribution was consistent with the Gaussian distribution. The X-ray powder diffraction (XRD) spectrum of Tris-CD (1 : 1) (Fig. S5†) exhibited three broad peaks centered at 2θ values of 13, 17.4 and 27.9°, corresponding to graphitic interlayer spacings of 6.7 Å, 4.9 Å and 3.2 Å, which can be attributed to highly disordered carbon species.[14] The various chemical bonds were confirmed by FT-IR analysis (Fig. 1b). The FT-IR spectra of Tris-CD (1 : 1) and EA-CD (1 : 1) exhibited peaks around 3420 cm^{-1} and 1210 cm^{-1}, which were assigned to the stretching and in-plane bending vibrations of the hydroxyl groups, respectively.[15] The FT-IR spectra indicated that hydroxyl groups were capped on the surface of Tris-CD (1 : 1) and EA-CD (1 : 1). X-ray photoelectron spectroscopy (XPS) was carried out to determine the composition of Tris-CDs and EA-CDs (Fig. 1c–h and S6†). Three peaks at 285.0, 400.0, and 533 eV were observed in the full XPS spectra of Tris-CDs and EA-CDs, as shown in Fig. S6,† which corresponded to C 1s, N 1s, and O 1s, respectively.[2f] C in four different chemical environments was clearly seen in the C 1s region as shown in the high resolution C 1s spectra (Fig. 1c and f), which corresponded to sp^2 C in C=C at 284.5 eV, sp^3 C in C–N at 285.8 eV, C–O at 286.6 eV, and C=O at 288.1 eV.[2f] The high-resolution N 1s spectra revealed two different types of nitrogen doping: pyrrolic nitrogen at about 398.2–399.5 eV, and graphitic nitrogen at about 400.5–401.5 eV (Fig. 1d and g).[12,16] The high-resolution O 1s spectra indicated two different types of oxygen bonds: C=O at 531.8 eV and C–O–C/C–O–H at 533.0 eV (Fig. 1e and h).[2f]

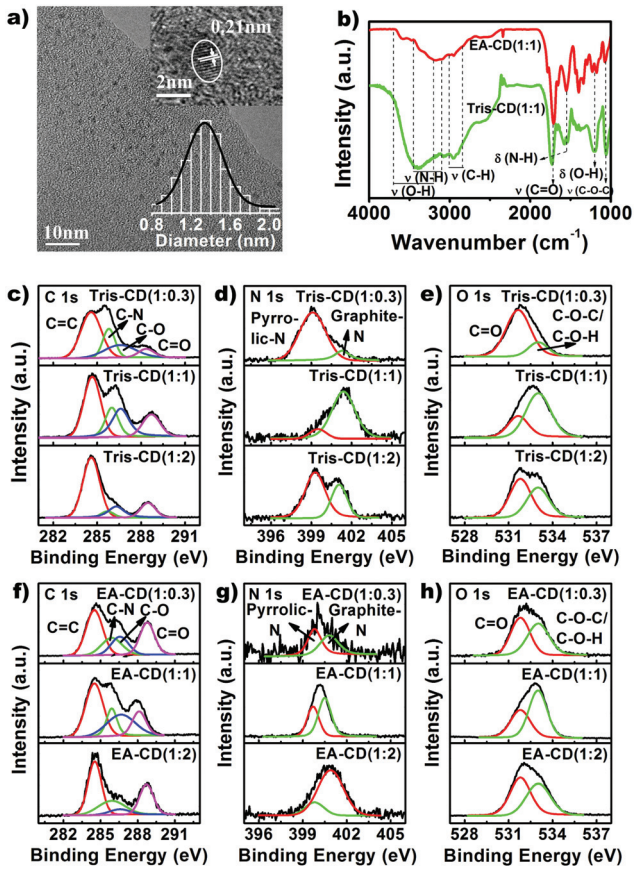

Fig. 1 (a) TEM image of Tris-CD (1 : 1) (upper inset figure is an HR-TEM image and the lower inset figure is the size distribution histogram of Tris-CD (1 : 1)). (b) The FT-IR spectra of Tris-CD (1 : 1) and EA-CD (1 : 1). The high resolution of (c) C 1s, (d) N 1s, and (e) O 1s XPS spectra of Tris-CD (1 : 0.3) (above), Tris-CD (1 : 1) (middle), and Tris-CD (1 : 2) (below). The high resolution of (f) C 1s, (g) N 1s, and (h) O 1s XPS spectra of EA-CD (1 : 0.3) (above), EA-CD (1 : 1) (middle), and EA-CD (1 : 2) (below).

The amounts of the different types of chemical bonds in Tris-CDs and EA-CDs are displayed in Table 1. The QYs, C–O and graphite-N content of Tris-CDs and EA-CDs, as a function of the molar ratio of the corresponding reactants are shown in Fig. 2. The maximum QY was obtained when the molar ratio of the corresponding reactants was 1 : 1, which corresponded to the greatest C–O and graphite-N content. Since carboxyl groups tend to react with amino groups more than hydroxyl under 700 W microwave radiation, the C–O bonds on the surface of Tris-CDs and EA-CDs primarily come from C–O–H moieties rather than C–O–C. This confirms that there are numerous hydroxyl groups on the surface of Tris-CD (1 : 1) and EA-CD (1 : 1). N-doped CDs (denoted as ED-CD) can be synthesized from CA and ED in the microwave oven. The QY of ED-CD (1 : 1) was 67.5% as determined by a slope method, while the QY of CDs without N-doping (synthesized using CA) was only 0.6% (Fig. S7 and Table S4†). However, carbonization did not occur during the reaction of CA and alcohols, such as ethanol, ethylene glycol, and 1,1,1-tris(hydroxylmethyl)ethane

Table 1 The amounts of various chemical bonds of Tris-CDs and EA-CDs in XPS spectra

	C 1s				N 1s	
Sample	C=C	C–N	C–O	C=O	Pyrrolic-N	Graphite-N
Tris-CD (1 : 0.3)	0.52	0.20	0.20	0.08	0.072	0.012
Tris-CD (1 : 1)	0.42	0.17	0.25	0.16	7.2×10^{-3}	0.055
Tris-CD (1 : 2)	0.65	0.06	0.15	0.14	0.074	0.036
EA-CD (1 : 0.3)	0.43	0.14	0.20	0.23	0.020	0.019
EA-CD (1 : 1)	0.46	0.11	0.24	0.19	0.034	0.050
EA-CD (1 : 2)	0.44	0.09	0.21	0.26	8.5×10^{-3}	0.040

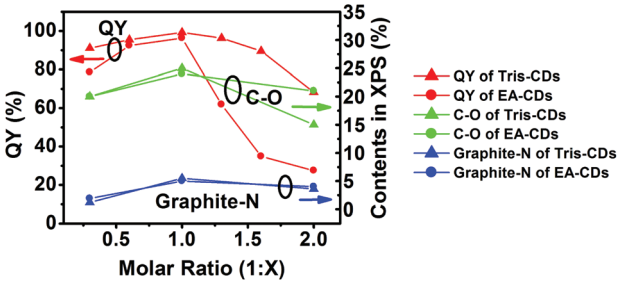

Fig. 2 QYs, C–O and graphite-N contents of EA-CDs and Tris-CDs as a function of molar ratio of the corresponding reactants.

under 700 W microwave radiation within 5 min, and fluorescent species were not detected in aqueous solutions. These results suggest that hydroxyl groups linked by C–O–C moieties on the surface of CDs hardly contribute to the QY. The XPS spectra of ED-CD (1 : 1) were also measured (Fig. S8 and Table S5†). The nitrogen doping was mainly attributed to graphitic nitrogen, which contributes to QY, as described previously.[2a,17] Graphitic nitrogen is similar to graphene, in which carbon is substituted with nitrogen atoms. A higher graphitic nitrogen content led to a higher QY, which was consistent with previous reports.[12,17] Graphitic nitrogen implies that most of the N-doping comes from the transformation from pyrrolic nitrogen and replacement of carbon atoms by nitrogen atoms. The aforementioned results indicate that Tris-CD (1 : 1) and EA-CD (1 : 1) present the maximum graphitic nitrogen and hydroxyl group content on their surfaces. Graphitic nitrogen and hydroxyl groups can result in enhanced luminescence.[12,15c,d,17] Although the mechanism of the interaction between hydroxyl groups and graphite nitrogen is unknown, we believe that the synergy leads to ultra-high QYs; this is the first report of CDs with ultra-high QYs due to the synergy between graphitic nitrogen and hydroxyl groups.

The Raman spectra of the CDs were obtained to further investigate the molecular structure (Fig. S9, S10, and Table S6†). The Raman spectra displayed two broad peaks at around 1380 cm^{-1} and 1610 cm^{-1}, which were attributed to the D-band (sp^3) and G-band (sp^2), respectively.[18] The D-band represents lattice defects in graphite, and the G-band represents the in-plane vibration of carbon atoms, so I_D/I_G corresponds to the degree of defects in CDs. The I_D/I_G was 1.03, 0.98, and 1.06 for Tris-CD (1 : 0.3), Tris-CD (1 : 1), and Tris-CD (1 : 2), respectively. The I_D/I_G was 1.38, 1.01, and 1.62 for EA-CD (1 : 0.3), EA-CD (1 : 1), and EA-CD (1 : 2), respectively. It seems that excessively high or low degrees of defects in CDs lead to low QYs, and only an appropriate degree of defects in CDs results in a high QY. Absolute QYs were also measured by using FLS920 and fit well with the results obtained using the slope method (Fig. S11†).

UV/Vis, PL, and fluorescence lifetime decay spectra

To further investigate the mechanism behind the high QYs, we obtained the UV/Vis, PL spectra, and PL decay curves of Tris-CDs, EA-CDs, and ED-CDs (Fig. 3, and S12, S13, S14, and S15†). In the UV/Vis spectra of Tris-CD (1 : 1), the former peak at 228 nm was assigned to the $\pi \rightarrow \pi^*$ transitions and the latter peak at 333 nm was assigned to the $n \rightarrow \pi^*$ transition, consistent with previous reports.[15e,19] Their excitation wavelength peaks appeared at 234 and 332 nm, and the PL emission peak appeared at 410 nm (Fig. 3a). The PL emission bands of Tris-CD (1 : 1) shifted when the excitation wavelength was varied (Fig. 3b), which is common in fluorescent carbon materials.[15c,d,17] In the UV/Vis spectrum of EA-CD (1 : 1), a clear peak appeared at 329 nm. The PL excitation spectrum shows two peaks at 241 and 336 nm, and the PL emission peak appears at 420 nm (Fig. 3c). The PL emission of EA-CD (1 : 1) was excitation-dependent (Fig. 3d). Previous reports indicated that the excitation-dependent PL behavior originated from the "giant red-edge effect", where hydroxyl moieties act as polar groups to dominate the fluorescence emission with an excitation wavelength-dependent behavior.[19c] The PL decay curves of Tris-CDs and EA-CDs were measured by a time-correlated single photon counting technique, and are shown in Fig. S13 and S14.† The lifetime (τ) of Tris-CD (1 : 1) was 14.73 ns (the maximum among Tris-CDs) and the QY was 99.3% (the maximum among Tris-CDs). This suggests that long-τ Tris-CDs have a higher QY, and short-τ Tris-CDs have a lower QY. The QYs of Tris-CD (1 : 0.3) and Tris-CD (1 : 2) were 91.1% and 68.3%, respectively (Tables S1 and S7†). EA-CDs and ED-CDs exhibited similar trends to the Tris-CDs in that the high QY CDs had a longer τ (Fig. S14, S15 and Tables S8, S9†).

The radiative transition rate (K_R) and non-radiative transition rate (K_{NR}) can be obtained from τ and Φ using the formulas $\tau = (K_R + K_{NR})^{-1}$ and $\Phi = K_R(K_R + K_{NR})^{-1}$, where Φ is the

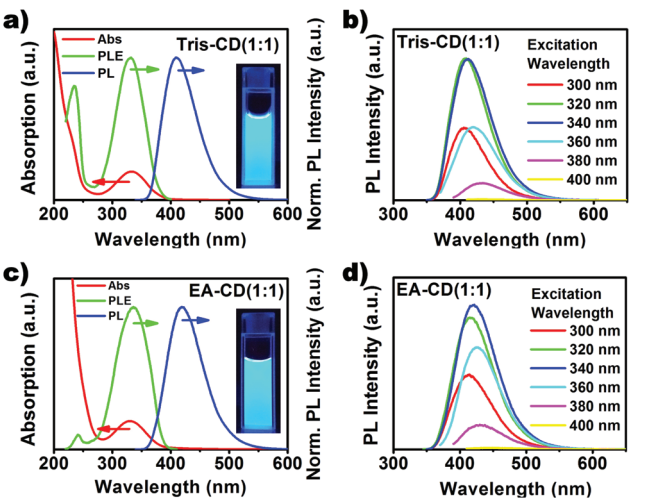

Fig. 3 UV/Vis absorption (red line), PL excitation (green line), and PL emission (blue line) spectra of (a) Tris-CD (1 : 1) and (c) EA-CD (1 : 1) in aqueous solutions, insets show the photographs of Tris-CD (1 : 1) and EA-CD (1 : 1) aqueous solutions under UV-light, respectively. PL emission spectra of (b) Tris-CD (1 : 1) and (d) EA-CD (1 : 1) aqueous solutions at excitation wavelengths of 300 nm (red), 320 nm (green), 340 nm (blue), 360 nm (cyan), 380 nm (magenta), and 400 nm (yellow).

QY and τ is the lifetime. The K_R and K_{NR} of EA-CDs, Tris-CDs, and ED-CDs are shown in Fig. 4 and Tables 1, 2 and S10.† In Fig. 4, the molar ratio is presented on the X axis and QY is on the Y axis; K_R is on the positive Z axis as it increases QY, and K_{NR} is on the negative Z axis as it decreases QY. As depicted in Fig. 4, the higher the top of the cylinder, and simultaneously, the further the bottom of the cylinder is from the XOY plane (or closer it is to the $z = 0$ plane), the higher the QY it affords. The degree of graphite-N and surface hydroxyl-functionalization, which increased K_R and decreased K_{NR}, was dependent on the molar ratio of the raw materials. When the molar ratio was varied from 1 : 0.3 to 1 : 1, the degree of graphite-N and surface hydroxyl-functionalization increased, which led to an increase in K_R and decrease in K_{NR}. In principle, the ratio of K_R and K_{NR} is the major determinant of QY among all kinds of CDs. QY is proportional to K_R/K_{NR}. The ratio of K_R and K_{NR} reached the highest level on the basis of the molar ratio being 1 : 1 (Tables 2 and 3). When the molar ratio was varied from 1 : 1 to 1 : 2, the degree of graphite-N and surface hydroxyl-functionalization decreased, which led to an decrease in K_R and increase in K_{NR}, and K_R/K_{NR} decreased gradually (Tables 2 and 3). The highest QY (99.3%) of Tris-CD (1 : 1) comes from a very high K_R/K_{NR} of 141.89 (Table 3), which originates from the synergy of the hydroxyl moieties and graphitic nitrogen. This indicates that CA and amino compounds containing hydroxyls are suitable reactants to effectively and quickly synthesize N-doped hydroxyl-functionalized CDs with highly fluorescent QYs in a simple microwave process.

We also evaluated the stability, resistance to photobleaching and zeta potential of the CDs. Fig. S16a† shows the PL intensity of Tris-CD (1 : 1) and EA-CD (1 : 1) to be 98% and 91% of the initial intensity respectively after two hours of sustained irradiation with a strong UV beam of 365 nm from a fluorescence spectrofluorometer (EX slit of 20 nm, photomultiplier of 700 V). The optical power density of the UV beam is 24.5 W cm^{-2}. Fig. S16b† shows the zeta potentials of Tris-CDs and EA-CDs, Tris-CD (1 : 1) and EA-CD (1 : 1) were the most stable in aqueous solutions.

Bioimaging was used to expand and validate the imaging applications of the ultra-high QY CDs. *Escherichia coli* (*E. coli*) cells (Gram-negative bacteria) at a concentration of ~10^8 cfu mL^{-1} were incubated with a 100 mg mL^{-1} Tris-CD (1 : 1) saline solution for 10 min (optimization of the concentration of Tris-CD (1 : 1) and staining time are shown in Fig. S17†). The cells were then separated and rinsed *via* centrifugation, and were subsequently fixed on a slide. After the slides were dried naturally, the mounting medium (glycerol : saline (9 : 1) solution) was dropped and stamped onto the slide. Then the slide was observed under an Olympus FV1000 confocal laser scanning microscope. As is shown in Fig. 5, the confocal fluorescence microscopy images exhibited bright blue fluorescence, and the

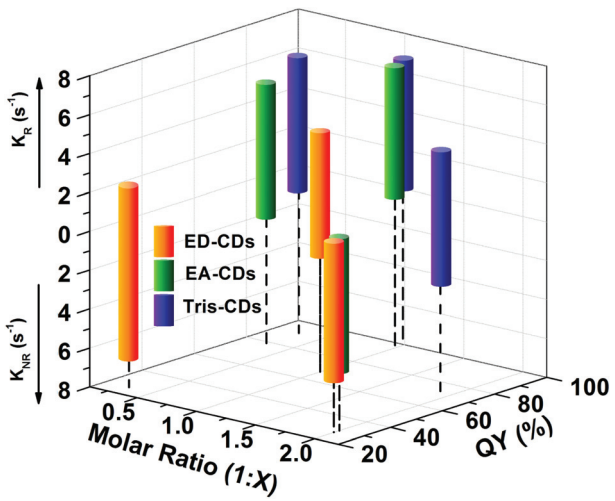

Fig. 4 K_R and K_{NR} against the QY and molar ratio of raw materials.

Table 2 τ, QY, K_R and K_{NR} of EA-CDs

Sample	EA-CD (1 : 0.3)	EA-CD (1 : 1)	EA-CD (1 : 2)
τ	14.54 ns	14.78 ns	13.74 ns
QY	78.6%	96.3%	27.4%
K_R (s^{-1})	5.41×10^7	6.52×10^7	1.99×10^7
K_{NR} (s^{-1})	1.47×10^7	2.5×10^6	5.28×10^7
K_R/K_{NR}	3.68	26.08	0.38

Table 3 τ, QY, K_R and K_{NR} of Tris-CDs

Sample	Tris-CD (1 : 0.3)	Tris-CD (1 : 1)	Tris-CD (1 : 2)
τ	14.40 ns	14.73 ns	14.28 ns
QY	91.1%	99.3%	68.3%
K_R (s^{-1})	6.33×10^7	6.74×10^7	4.78×10^7
K_{NR} (s^{-1})	6.18×10^6	4.75×10^5	2.22×10^7
K_R/K_{NR}	10.24	141.89	2.15

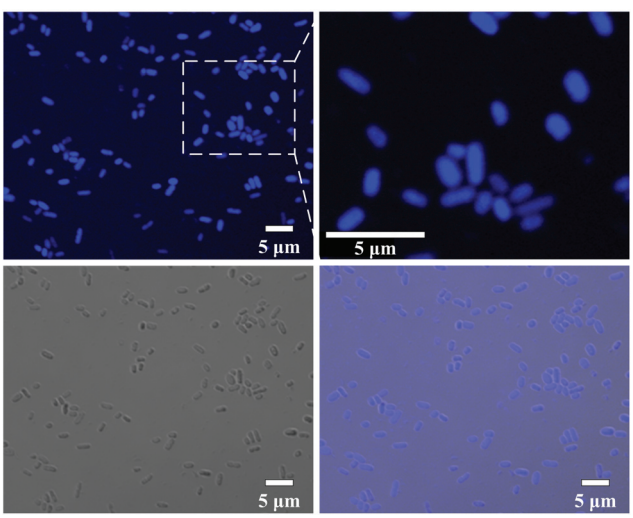

Fig. 5 Confocal fluorescence microscopy images of *E. coli* cells stained with Tris-CD (1 : 1); the image under 405 nm light excitation (above left), the enlarged partial view (above right), the image under bright field (lower left) and the combination images under 405 nm light excitation and bright field (lower right).

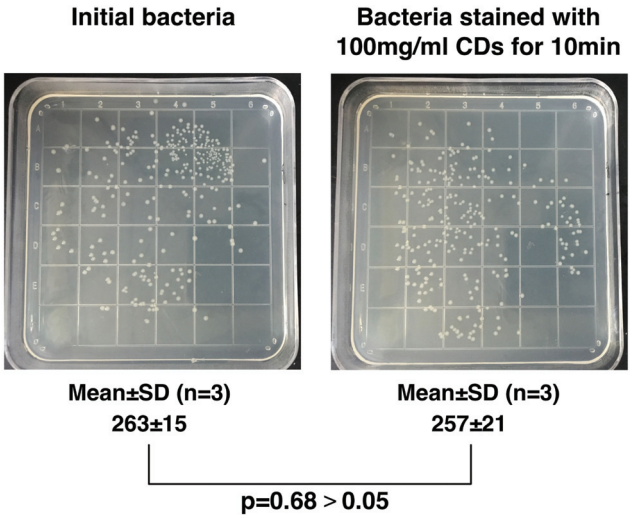

Fig. 6 The biocompatibility and toxicity of Tris-CD (1 : 1) were evaluated by the plate counting method. The suspension of 10^8 cfu ml^{-1} live *E. coli* was divided into six parts with three stained with 100 mg ml^{-1} Tris-CD (1 : 1) for 10 min (stained bacteria) and the other incubated with saline for 10 min (initial bacteria). The bacteria in six suspensions were collected by centrifuging and washing twice with saline, respectively. Then six samples of bacteria were diluted to about 10^3 cfu ml^{-1} with 200 μl of each for plate counting. Then, the bacteria were grown in Luria–Bertani (LB) medium at 37 °C for 12 h for plate counting.

enlarged partial view illustrates that Tris-CD (1 : 1) can penetrate *E. coli* cells, which were stained homogeneously within a short staining time of 10 min. The biocompatibility and toxicity of Tris-CD (1 : 1) were evaluated by the plate counting method (Fig. 6). The data of plate counting indicated that there was no significant difference (p = 0.68 > 0.05, T-test) of cell viability between the initial bacteria and the stained ones with 263 ± 15 counted live bacteria and 257 ± 21 for the two. These results demonstrate that Tris-CD (1 : 1) is a promising low-toxicity fluorescence staining agent for bioimaging applications.

Conclusions

In summary, a facile method for the microwave synthesis of a series of CDs with QYs as high as 99% was developed. CA was selected as the carbon source because it can easily form a graphene framework through intermolecular dehydration. Amino compounds containing hydroxyl groups can easily provide N-doping and strong electron-donating hydroxyl moieties. The synergy between the hydroxyl moieties and graphitic nitrogen can give rise to a much improved radiative transition rate and ultra-high QY. The QYs of the resulting CDs exceeded 99% when the molar ratio between CA and the other component was 1 : 1. The developed process provides a simple and efficient method to synthesize CDs with high QYs, which may promote novel applications of CDs. In addition, the ultra-high QY Tris-CD (1 : 1) turned out to be a promising low-toxicity fluorescence staining agent.

Acknowledgements

This work was funded by the Innovation Program of Chinese Academy of Sciences (CAS), the National Natural Science Foundation of China No. 51503196, the Jilin Province Science and Technology Research Project No. 20140520119JH and 20150101039JC, and a project supported by the State Key Laboratory of Luminescence and Applications.

Notes and references

1 (*a*) J. Liu, Y. Liu, N. Liu, Y. Han, X. Zhang, H. Huang, Y. Lifshitz, S.-T. Lee, J. Zhong and Z. Kang, *Science*, 2015, **347**, 970; (*b*) H. Li, X. He, Z. Kang, H. Huang, Y. Liu, J. Liu, S. Lian, C. H. A. Tsang, X. Yang and S.-T. Lee, *Angew. Chem., Int. Ed.*, 2010, **49**, 4430.

2 (*a*) S. Zhu, Q. Meng, L. Wang, J. Zhang, Y. Song, H. Jin, K. Zhang, H. Sun, H. Wang and B. Yang, *Angew. Chem., Int. Ed.*, 2013, **125**, 4045; (*b*) L. Zhou, Y. Lin, Z. Huang, J. Ren and X. Qu, *Chem. Commun.*, 2012, **48**, 1147; (*c*) Y. Wang, L. Zhang, R.-P. Liang, J.-M. Bai and J.-D. Qiu, *Anal. Chem.*, 2013, **85**, 9148; (*d*) H. X. Zhao, L. Q. Liu, Z. D. Liu, Y. Wang, X. J. Zhao and C. Z. Huang, *Chem. Commun.*, 2011, **47**, 2604; (*e*) W. Wei, C. Xu, J. Ren, B. Xu and X. Qu, *Chem. Commun.*, 2012, **48**, 1284; (*f*) S. Liu, J. Tian, L. Wang, Y. Zhang, X. Qin, Y. Luo, A. M. Asiri, A. Al-Youbi and X. Sun, *Adv. Mater.*, 2012, **24**, 2037.

3 (*a*) W. F. Zhang, H. Zhu, S. F. Yu and H. Y. Yang, *Adv. Mater.*, 2012, **24**, 2263; (*b*) H. Zhu, W. Zhang and S. F. Yu, *Nanoscale*, 2013, **5**, 1797.

4 (*a*) F. Wang, Y. Chen, C. Liu and D. Ma, *Chem. Commun.*, 2011, **47**, 3502; (*b*) X. Zhang, Y. Zhang, Y. Wang, S. Kalytchuk, S. V. Kershaw, Y. Wang, P. Wang, T. Zhang, Y. Zhao, H. Zhang, T. Cui, Y. Wang, J. Zhao, W. W. Yu and A. L. Rogach, *ACS Nano*, 2013, **7**, 11234.

5 Y. Li, Y. Hu, Y. Zhao, G. Shi, L. Deng, Y. Hou and L. Qu, *Adv. Mater.*, 2011, **23**, 776.

6 (*a*) L. Cao, X. Wang, M. J. Meziani, F. Lu, H. Wang, P. G. Luo, Y. Lin, B. A. Harruff, L. M. Veca, D. Murray, S.-Y. Xie and Y.-P. Sun, *J. Am. Chem. Soc.*, 2007, **129**, 11318; (*b*) Y.-P. Sun, B. Zhou, Y. Lin, W. Wang, K. A. S. Fernando, P. Pathak, M. J. Meziani, B. A. Harruff, X. Wang, H. Wang, P. G. Luo, H. Yang, M. E. Kose, B. Chen, L. M. Veca and S.-Y. Xie, *J. Am. Chem. Soc.*, 2006, **128**, 7756; (*c*) S.-T. Yang, X. Wang, H. Wang, F. Lu, P. G. Luo, L. Cao, M. J. Meziani, J.-H. Liu, Y. Liu, M. Chen, Y. Huang and Y.-P. Sun, *J. Phys. Chem. C*, 2009, **113**, 18110.

7 D.-Y. Guo, C.-X. Shan, S.-N. Qu and D.-Z. Shen, *Sci. Rep.*, 2014, **4**, 7469.

8 (*a*) Y. Dong, H. Pang, H. B. Yang, C. Guo, J. Shao, Y. Chi, C. M. Li and T. Yu, *Angew. Chem., Int. Ed.*, 2013, **52**, 7800; (*b*) H. Sun, L. Wu, N. Gao, J. Ren and X. Qu, *ACS Appl. Mater. Interfaces*, 2013, **5**, 1174; (*c*) H. Zheng, Q. Wang, Y. Long, H. Zhang, X. Huang and R. Zhu, *Chem. Commun.*, 2011, **47**, 10650.

9 (*a*) L.-L. Li, J. Ji, R. Fei, C.-Z. Wang, Q. Lu, J.-R. Zhang, L.-P. Jiang and J.-J. Zhu, *Adv. Funct. Mater.*, 2012, **22**, 2971; (*b*) S. Zhu, J. Zhang, S. Tang, C. Qiao, L. Wang, H. Wang, X. Liu, B. Li, Y. Li, W. Yu, X. Wang, H. Sun and B. Yang, *Adv. Funct. Mater.*, 2012, **22**, 4732; (*c*) X. Wang, Y. Long, Q. Wang, H. Zhang, X. Huang, R. Zhu, P. Teng, L. Liang and H. Zheng, *Carbon*, 2013, **64**, 499.

10 J. Shen, Y. Zhu, C. Chen, X. Yang and C. Li, *Chem. Commun.*, 2010, **47**, 2580.

11 D. K. Palit, H. Pal, T. Mukherjee and J. P. Mittal, *J. Chem. Soc., Faraday Trans.*, 1990, **86**, 3861.

12 D. Qu, M. Zheng, L. Zhang, H. Zhao, Z. Xie, X. Jing, R. E. Haddad, H. Fan and Z. Sun, *Sci. Rep.*, 2014, **4**, 5294.

13 (*a*) Y. Dong, J. Shao, C. Chen, H. Li, R. Wang, Y. Chi, X. Lin and G. Chen, *Carbon*, 2012, **50**, 4738; (*b*) D. Qu, M. Zheng, P. Du, Y. Zhou, L. Zhang, D. Li, H. Tan, Z. Zhao, Z. Xie and Z. Sun, *Nanoscale*, 2013, **5**, 12272.

14 S. Qu, X. Wang, Q. Lu, X. Liu and L. Wang, *Angew. Chem., Int. Ed.*, 2012, **124**, 12381.

15 (*a*) L. Liu, Y. Li, L. Zhan, Y. Liu and C. Huang, *Sci. China: Chem.*, 2011, **54**, 1342; (*b*) A. Khanam, S. K. Tripathi, D. Roy and M. Nasim, *Colloids Surf., B*, 2013, **102**, 63; (*c*) X. Zhai, P. Zhang, C. Liu, T. Bai, W. Li, L. Dai and W. Liu, *Chem. Commun.*, 2012, **48**, 7955; (*d*) D. Pan, J. Zhang, Z. Li, C. Wu, X. Yan and M. Wu, *Chem. Commun.*, 2010, **46**, 3681; (*e*) M. Li, S. K. Cushing, X. Zhou, S. Guo and N. Wu, *J. Mater. Chem.*, 2012, **22**, 23374.

16 Z.-H. Sheng, L. Shao, J.-J. Chen, W.-J. Bao, F.-B. Wang and X.-H. Xia, *ACS Nano*, 2011, **5**, 4350.

17 J. Sun, S. Yang, Z. Wang, H. Shen, T. Xu, L. Sun, H. Li, W. Chen, X. Jiang, G. Ding, Z. Kang, X. Xie and M. Jiang, *Part. Part. Syst. Charact.*, 2015, **32**, 434.

18 (*a*) M. Lee, S. K. Balasingam, H. Y. Jeong, W. G. Hong, H.-B.-R. Lee, B. H. Kim and Y. Jun, *Sci. Rep.*, 2015, **5**, 8151; (*b*) A. M. Llyin, N. R. Guseinov, I. A. Tsyganov and R. R. Nemkaeva, *Phys. E*, 2011, **43**, 1262.

19 (*a*) K. P. Loh, Q. Bao, G. Eda and M. Chhowalla, *Nat. Chem.*, 2010, **2**, 1015; (*b*) C. Galande, A. D. Mohite, A. V. Naumov, W. Gao, L. Ci, A. Ajayan, H. Gao, A. Srivastava, R. B. Weisman and P. M. Ajayan, *Sci. Rep.*, 2011, **1**, 85; (*c*) S. K. Cushing, M. Li, F. Huang and N. Wu, *ACS Nano*, 2013, **8**, 1002.